IOSR Journal of Applied Physics (IOSR-JAP)
e-ISSN: 2278-4861.Volume 6, Issue 2 Ver. III (Mar-Apr. 2014), PP 15-20
www.iosrjournals.org

Numerical simulation of $In_xGa_{1-x}N$ single junction solar cells using AMPS-1D

A. K. Das
Department of Physics, P. K. College, Contai; Contai-721401, India.

Abstract: *The solar cell structure based on indium gallium nitride (InGaN) as the absorber layer is simulated using the one dimension (1D) simulation program 'Analysis of Microelectronic and Photonic Structures' (AMPS) that was initially developed at the Pennsylvania State University, USA. In this paper, I have used the global air mass AM 1.5G (one sun) illumination (100mW/cm^2, 0.30μm-1.1μm) to calculate the optimum efficiency of single junction solar cells with different band gap energy (E_g) varies from 1.12eV to 1.92eV by varying mole fraction (x) of In with and without un-doped (i) layer between p and n layers of the cell. The optimal efficiencies of $In_xGa_{1-x}N$ solar cells are obtained, respectively, 28.088% without i-layer for x (0.62) corresponding to E_g of 1.40 eV and for the total device thickness (L) of 400 nm and 27.411% with i-layer of same x incorporating between p and n layers of the cell of x (0.46) corresponding to E_g of 1.80 eV and for lowering L to 290 nm by considering high quality InGaN. In the simulation, the current density-voltage (J-V) characteristics are performed by varying E_g and the quantum efficiency by varying L from 400 nm to 4000 nm.*
Keywords - *AMPS-1D simulation, conversion efficiency, InGaN thin film, solar cell, quantum efficiency*

I. Introduction

InGaN is one of the most promising direct band gap ternary Group III-V (nitrides) semiconductor-alloy materials as an absorber for high efficiency thin film solar cells. These materials have recently drawn intensive research interest due to their tunable band gap energy range of 0.7 to 3.4eV, which is applicable to the entire functional range of the solar spectrum. Group III-nitrides have the advantages of high absorption co-efficient, high carrier mobility, high drift velocity, high radiation resistance, as well as high thermal conductivity. These properties contribute to the potential of InGaN based solar cells for use in harsh environments, especially for space and terrestrial applications.

Also indium-rich InGaN solar cell can be fabricated ultrathin consuming much less material and has greater conversion efficiency than the commonly used germanium or silicon solar cells that have the optimum efficiency not more than 24%. Low In content InGaN materials are successfully used in the fabrication of blue light emitting diodes, blue laser diodes and UV detectors; these give the technological support for research of high In content InGaN solar cells. However, the growth of high quality, high In content InGaN material still encounter some difficulties, such as phase separation, high InN pressure, P type doping, lattice matching.

Jani et al. [1] designed low In content $In_xGa_{1-x}N$ ($x = 0.04{\sim}0.05$) pin and quantum well solar cells and characterized them. Xiaobin Zang et al [2] reported the optimum efficiency (20.284%) of single junction solar cells of 65% In content using AMPS-1D. Hamzaoui et al [3] analyzed InGaN solar cells with up to six junctions getting preliminary results concerning the relationship of open circuit voltage and short circuit current density variation with the junction numbers. Tae Hoon Seo et al [4] have recently fabricated low In (15%) content $In_{0.15}Ga_{0.85}N$ -based multiple quantum well (MQW) solar cell as absorbing layer between p-GaN and n-GaN of band gap of 3.40 eV and improved photovoltaic effects using graphene network on indium tin oxide (ITO) nanodots as anti-reflecting coating (ARC) on p-GaN epilayer. However, the fabrication of high In content InGaN solar cell is now challenging.

II. Simulation Model

The theoretical calculations carried out using AMPS-1D (Fig. A) for the analysis were based on Poisson's equation and the first-principle continuity equations of electrons and holes [5] and used to analyze the carriers transport behavior of semiconductor electronic and optoelectronic device structures including solar cells.

In one dimension case, Poisson's equation is written as;

$$\frac{d}{dX}\left(-\varepsilon(X)\frac{d\Psi}{dX}\right) = q * [p(X) - n(X) + N_D^+(X) - N_A^-(X) + p_t(X) - n_t(X)] \quad (1)$$

where the electrostatic potential Ψ, the free electron n , free hole p , trapped electron n_t, and trapped hole p_t as well as the ionized donor-like doping N_D^+ and ionized acceptor-like doping N_A^- concentrations are all functions of the position co-ordinate X. Here, ε is the permittivity and q is the magnitude of charge of an electron. The

continuity equations for the free electrons and holes in the delocalized (band) states of the conduction band and valence band, respectively, have the forms:

for electron ; $\frac{1}{q}\left(\frac{dJ_n}{dX}\right) = -G_{op}(X) + R(X)$ (2)

and for hole; $\frac{1}{q}\left(\frac{dJ_p}{dX}\right) = G_{op}(X) - R(X)$ (3)

where J_n and J_p are, respectively, the electron and hole current densities. The term $R(X)$ is the net recombination rate resulting from direct band-to-band recombination and indirect Shockley-Read-Hall (SRH) recombination through gap (localized) states and the term $G_{op}(X)$ is the optical generation rate as a function of X due to externally imposed illumination.

The AMPS-1D can operate in two distinct modes: the density of state (DOS) mode or the lifetime mode. The DOS mode allows the definition of multiple defect states using densities, energy distribution, and capture cross-sections. The lifetime model does not allow the said recombination processes, where inputs are given in the form of carrier life times, which are assumed constant, independent of light and voltage bias. In this work, I use the DOS mode in the simulation of InGaN solar cells.

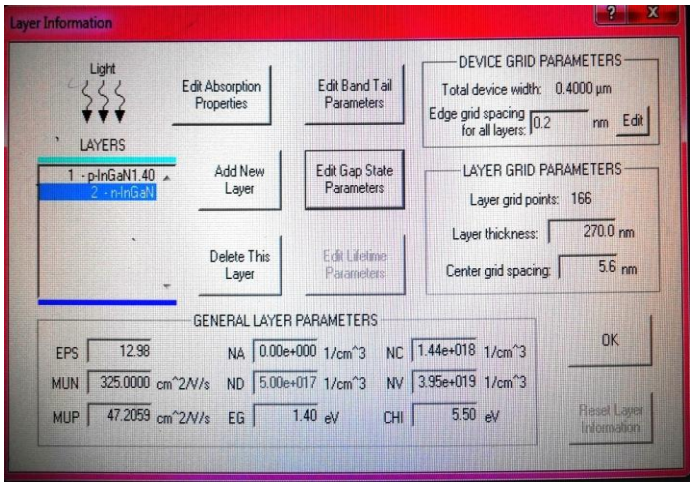

Figure A AMPS simulation front panel contains the device and layer grid parameters and general layer parameters

III. Parametric Equations for Simulation at Temperature, T = 300 K

Band gap [6] in eV; $E_g(x) = 0.7x + 3.4(1-x) - 1.43(1-x)$ (i)

where, x be the mole fraction.

Absorption co-efficient [2] $in\ \mu m^{-1}$; $\alpha(\lambda, E_g) = A\sqrt{\frac{1.2398}{\lambda} - E_g}$ (ii)

where, λ be the wave length in μm and $A = 2.2 \times 10^5\ \mu m^{-1}\ (eV)^{-\frac{1}{2}}$

Electron affinity [2, 7] $in\ eV$; $\chi(E_g) = 4.1 + 0.7(3.4 - E_g)$ (iii)

Relative permittivity [7]; $\varepsilon_r(x) = 14.6x + 10.4(1-x)$ $^{\varkappa}$ (iv)

Effective density of states in the conduction band [7] and valence band [7], respectively, $in\ cm^{-3}$;

$N_c(x) = 0.9x + 2.3(1-x)$ $^{\varkappa}$ (v)

$and;\ N_v(x) = 5.3x + 1.8(1-x)$ $^{\varkappa}$ (vi)

Carrier mobility [8] $in\ cm^2V^{-1}s^{-1}$; $\mu_i(\mathcal{N}) = \mu_{min,i} + \frac{\mu_{max,i} - \mu_{min,i}}{1 + (\frac{\mathcal{N}}{\mathcal{N}_{g,i}})^{\gamma_i}}$ (vii)

The carrier mobility of InGaN is assumed similar to GaN, where $i = n, p$ denotes electrons and holes, respectively, and $\mathcal{N}$ be the doping concentration, while the model parameters $\mu_{max,i}$, $\mu_{min,i}$, $\mathcal{N}_{g,i}$ and γ_i depend on the type of semiconductor [8]. In addition, the $\varkappa$ marked equations are obtained from the linear fitting of the corresponding parameters of InN and GaN.

IV. Cell Parameters of the $In_xGa_{1-x}N$ Solar Cells

Table 1 Model parameters used in the calculation of the mobility

Type of carriers	$\mu_{max,i}(cm^2V^{-1}s^{-1})$	$\mu_{min,i}(cm^2V^{-1}s^{-1})$	$N_{g,i}(cm^{-3})$	γ_i
electron	10^3	55	2×10^{17}	1
hole	170	3	3×10^{17}	2

Table 2 Parameters for the simulation of $In_xGa_{1-x}N$ single junction solar cells (a) without i-layer and (b) with i-layer

SCs type	Layer	x (%)	E_g (eV)	χ (eV)	N_c $\times10^{18}$ (cm^{-3})	N_v $\times10^{19}$ (cm^{-3})	ε_r	N_D $\times10^{17}$ (cm^{-3})	N_A $\times10^{17}$ (cm^{-3})	μ_n $(cm^2 V^{-1} s^{-1})$	μ_p $(cm^2 V^{-1} s^{-1})$
(a)	p	62	1.4	5.50	1.44	3.95	12.98	0	5	325	47.2
	n							5	0		
(b)	p	46	1.8	5.22	1.65	3.41	12.33	0	5		
	i	62	1.4	5.50	1.44	3.95	12.98	0	0		
	n	46	1.8	5.22	1.65	3.41	12.33	5	0		

Surface recombination velocity (SRV) [9] of electrons and holes are same and is equal to 1×10^3 cm/s and reflection co-efficient 0.05[11] and 0.99, respectively, for front and back surfaces of the cell.

V. Cell Structures

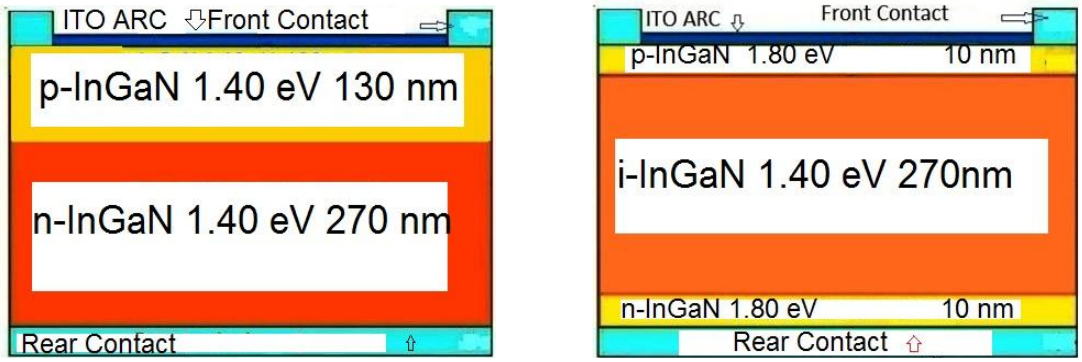

Figure 1 schematic diagram of InGaN single junction solar cells structures: (a) without i- layer (b) with i-layer

VI. Results and Discussions

In this paper, several $In_xGa_{1-x}N$ single junction solar cells are designed with moderate and low concentrations of indium (In) varying from $42\% - 74\%$. The photo-generated short-circuit current density (J_{SC}) and the open-circuit voltage (V_{OC}) of each structure under $AM\ 1.5G$ illumination of photon flux from ASTM G173-03 [11] are simulated for different cell thickness in order to find the key parameters for the fabrication of $In_xGa_{1-x}N$ solar cells with optimum efficiency. The fill factor (FF) in conjunction with $V_{OC}$and J_{SC} determines the maximum power $(V_{mp}J_{mp})$ from the solar cell which is defined as the ratio of the product of V_{mp} and J_{mp} to the product of $V_{OC}$and J_{SC} of the cell i.e. $FF = \frac{V_{mp}J_{mp}}{V_{OC}Jsc}$ and in addition, the conversion efficiency $(\eta) = \frac{V_{mp}\,Jmp}{P_{in}}$, where P_{in} be the incident power of photon on the solar cell under one sun illumination.

Effect of band gap on performance of $In_xGa_{1-x}N$ solar cells

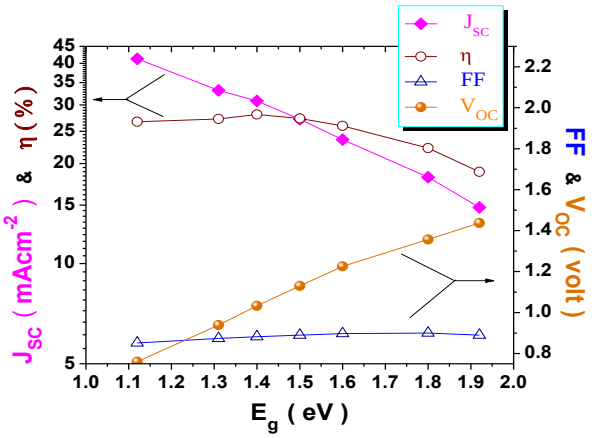

Figure 2 variations of η and J_{SC}; V_{OC} and FF as a function of band gap (E_g)

Fig. 2 shows single junction solar cell performances as a function of E_g without i-layer between p and n layers of the cell as Fig. 1(a). It is observed that V_{OC} and FF increase with E_g varying from 1.12 $eV - 1.92eV$ except at 1.92 eV where the later curve decreases. Also the curve containing η shows less increment with decrease in E_g by raising In concentration in $In_xGa_{1-x}N$ solar cell than J_{SC} which is optimum at 1.40 eV corresponding to x about 62% (Table 2(a)) and for p and n-layers thicknesses, respectively,130 nm and 270 nm . Then the curve drops by further decrease of E_g .

Fig. 3 shows the same performances as Fig. 2 but here an i-layer of E_g varying from 1.12 eV to 1.5 eV is incorporated between p and n layers each of 10 nm thick and band gap 1.80 eV as Fig. 1(b) so that the η becomes optimum. The graphs of J_{SC} and V_{OC} show the same nature as in Fig. 2 except the η , which is optimum at 27.411% for i-$In_{0.62}Ga_{0.38}N$ layer of E_g of 1.40 eV and by lowering the total device thickness (L) to 290 nm in expense of a part of FF and J_{SC} by 2.04% and 0.93%, respectively.

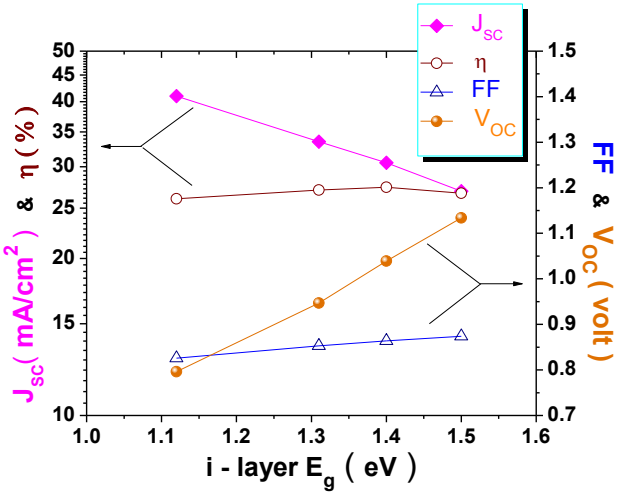

Figure 3 variations of η and J_{SC}; V_{OC} and FF as a function of i- layer E_g.

J-V characteristics of the cells

The Fig. 4 shows the J- V characteristics of $InGaN$ solar cells for the L of 400 nm using AMPS-1D. It is observed that the curve for lower $E_g(1.12eV)$ shows higher J_{SC} at significantly low V_{OC} , results lesser efficiency unlike others two where they have higher V_{OC} with moderate J_{SC} and give ultimate optimum η (≈28%) at E_g of 1.40 eV.

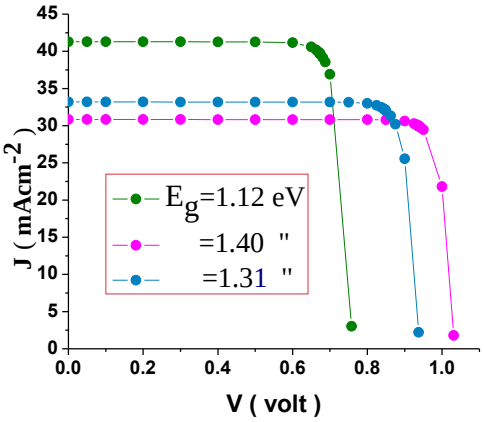

Figure 4 J-V characteristics of InGaN solar cells without i-layer as a parameter of band gap (E_g)

Quantum efficiency as a function of cell thickness

The term quantum efficiency (QE) of the solar cell is defined as the ratio of the number of minority carriers collected by the cell to the number of photons of a given energy incident on the cell. If all photons of certain energy are absorbed and the resulting minority carriers are collected, then the quantum efficiency at that particular energy is unity. The quantum efficiency for photons with energy below the band gap is zero.

Fig. 5 shows the such QE spectra of the cell of E_g=1.40 eV as a parameter of L (400-4000 nm) by varying n-layer thickness for high SRV of 1.0×10^7 cm.s^{-1} of electrons and holes at the front and back surfaces of the device. It can be observed that for higher thickness, the cell shows broader QE spectra, results the absorption of more photons which improves the overall efficiency (Fig. 6) of the solar cells unlike at lower SRV ($\sim10^3$cms^{-1}, for good surface passivation) where no improvement of η, rather it slightly decreases due to bulk recombination. The QE spectra for higher thicknesses of the cell, are not only broader but also closer, reveal the no significant change of the curves and hence in the conversion efficiencies exceeding the cell thickness of 3000 nm. In the figure, the pink curve for cell thickness 4000 nm merges the green curve (not seen in Fig. 5) for L of 3000nm. In addition, the QE is about 0.94 for 95% absorption of incident photon of wavelength (λ) of 0.58 μm by using efficient anti-reflecting coating (ARC) [10] on the front surface of the cell. There are also sharp decrements of QE for lower and higher λ in solar spectrum, respectively, due to front surface recombination (not shown in the Fig. 5) and rear surface recombination as well as small absorptions of photons near the band edge ($\lambda\sim0.88$ μm).

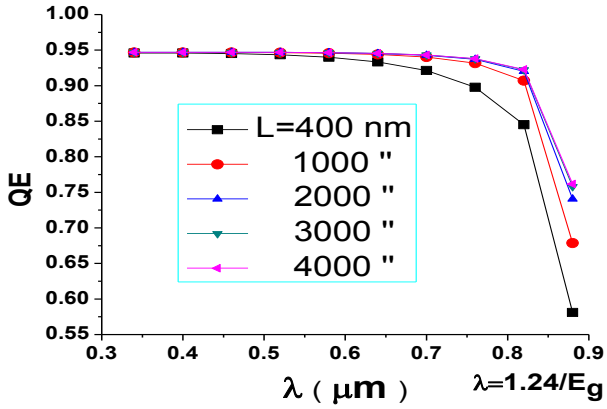

Figure 5 QE spectra for different InGaN thickness (L) shows that higher thickness absorbs more photons which improves the overall efficiency of the device

Open circuit voltage, short circuit current and efficiency as a function of cell thickness

Fig. 6 shows the variation in the V_{OC} and J_{SC} including η as a function of cell thickness. It indicates that below $L = 1000$ nm, the cell shows the sharp decrease in the V_{OC}, J_{SC} and therefore decrease in the η.

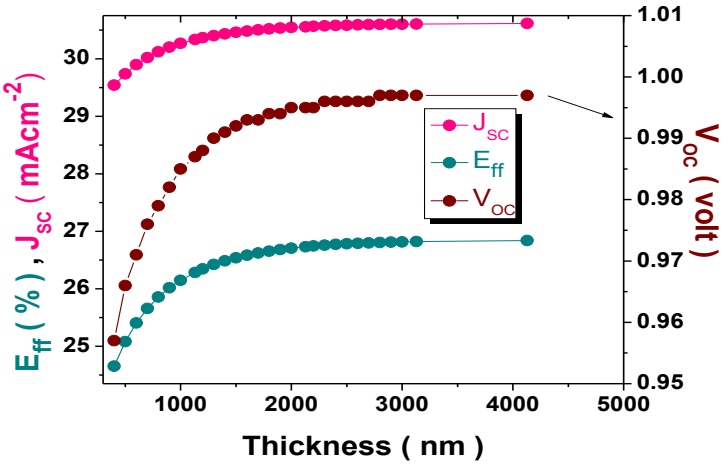

Figure 6 variations of V_{OC}, J_{SC} *and* η as a function of L

VII. Conclusion

The optimum performance of the $In_{0.62}Ga_{0.38}N$ single junction solar cell is simulated by AMPS-1D to study the dependence on band gap and on absorber layer thickness. Optimum efficiency is obtained as 28.088% at band gap of 1.40 eV for cell thickness of 400 nm. In addition, the efficiency can be optimized by lowering total device thickness by incorporating un-doped layer between p-n layers and using low band gap layers towards the rear surface of the cell. It is also observed that the conversion efficiency increased until the

thickness reached at around 3000 nm for high SRV. Similarly, the response of QE is nearly overlapped after 3000 nm thickness of the solar cell.

Acknowledgement

I would like to acknowledge the use of AMPS-1D program that was developed by Dr. Fonash's group at Pennsylvania State University (PSU).

References

[1] Jani, O., Ferguson, I., Honsberg, C., Kurtz, S., "Design and characterization of GaN/InGaN solar cells," *Appl. Phys.Lett., 91*, 2007, 132117.
[2] Xiaobin Zhang et al, "Simulation of In0.65Ga0.35 N single-junction solar cell" *J. Phys. D: Appl. Phys., 40*, 2007, 7335–7338.
[3] Hamzaoui, H., Bouazzi, A. S. and Rezig, B., "Theoretical possibilities of InxGa1-xN tandem PV structures," *Sol. Energy Mater. Sol. Cells 87*, 2005, 595-603.
[4] Tae Hoon Seo et al., "Improved photovoltaic effects in InGaN-based multiple quantum well solar cell with graphene on indium tin oxide nanodot nodes for transparent and current spreading electrode" *Appl. Phys. Lett., 102*, 2013, 031116.
[5] Fonash, S. et al., *http://www.cneu.psu.edu/amps/*.
[6] Wu, J., Walukiewicz, W., Yu, K. M., Ager III, J. W., Haller, E. E., Lu, H., Schaff, W. J., Saito, Y. and Nanishi, Y., "Unusual properties of the fundamental band gap of InN," *Appl. Phys. Lett., 80*, 2002, 3967-3969.
[7] Levinshtein, M. E., Rumyantsev, S. L. and Shur, M. S., *Properties of Advanced Semiconductor Materials*, (Wiley, Chichester, UK, 2001, 1–90).
[8] Mnatsakanov, T. T., Levinshtein, M. E., Pomortseva, L. I.,Yurkov, S. N., Simin, G. S. and Asif Khan, M., "Carrier mobility model for GaN" *Solid-State Electron. 47*, 2003, 111-115.
[9] Aleksiejūnas, R. et al., "Carrier transport and recombination in InGaN/GaN heterostructures, studied by optical four-wave mixing technique" *Phys. Status Solidi (c) 0*, 2003, 2686.
[10] ASTM G173-03 Reference Spectra Derived from SMARTS v. 2.9.2, "Reference Solar Spectral Irradiance: Air Mass 1.5 G" *http://www.rredc.nrel.gov /solar /spectra /am1.5*/.
[11] Dong-Ju Seo et al., "Efficiency improvement in InGaN-based solar cells by indium tin oxide nano dots covered with ITO films" *Optical Society of America 20, .S6 / Optics Express A991*, 2012.